Available online at www.sciencedirect.com

ScienceDirect

journal homepage: www.elsevier.com/locate/issn/15375110

Research Paper

The accuracy and utility of a low cost thermal camera and smartphone-based system to assess grapevine water status

Paul R. Petrie [a,*], Yeniu Wang [b], Scarlett Liu [c,d], Stanley Lam [c], Mark A. Whitty [c], Mark A. Skewes [b]

[a] South Australian Research and Development Institute and the Australian Wine Research Institute, Waite Campus, Urrbrae, SA, Australia
[b] South Australian Research and Development Institute, Loxton Research Centre, Loxton, SA, Australia
[c] School of Mechanical and Manufacturing Engineering, University of New South Wales, Sydney, NSW, Australia
[d] School of Traffic and Transportation Engineering, Central South University, Changsha, Hunan, China

ARTICLE INFO

Article history:
Received 23 May 2018
Received in revised form
22 December 2018
Accepted 9 January 2019
Published online 31 January 2019

Keywords:
Infrared thermometry
Irrigation scheduling
Reference surfaces
Stomatal conductance
Stem water potential
Smartphone application

Smartphones have several advantages over specialist monitoring systems including ubiquity, price, and ease of implementing updates. Thermal imaging can be used to assess plant water status and allow more informed irrigation decisions; unfortunately, this technique has not been widely adopted due to the high cost of equipment and the lack of a system to provide analysis and results in real-time. Several inexpensive thermal cameras that connect to smartphones have recently been released and one of these (FLIR One) was evaluated as part of a system to assess grapevine water status. Irrigation treatments were established on Cabernet Sauvignon and Chardonnay vines in an arid region. Thermal images were taken from the shaded side of the grapevine canopy and software was developed to automatically determine the temperature of the canopy and artificial reference leaves. The temperature readings and metrological inputs were used to calculate five indices of water status including the Crop Water Stress Index (CWSI) and the stomatal conductance index. The best performing was the CWSI, which does not require input from a weather station. Over 30 days of assessment, and a range of irrigation levels, measurements collected with the thermal camera were correlated with stem water potential ($R^2 = 0.61$) and stomatal conductance ($R^2 = 0.74$). Windy conditions appeared to be the major cause of variation between CWSI and stomatal conductance. Inexpensive thermal cameras have the potential to be an easy and accessible tool for the assessment of plant water status and to make better irrigation decisions.

* *Corresponding author*. South Australian Research and Development Institute, G.P.O. Box 397, Adelaide, SA 5001, Australia.
E-mail address: paul.petrie@sa.gov.au (P.R. Petrie).
https://doi.org/10.1016/j.biosystemseng.2019.01.002

Nomenclature

CWSI	Crop water stress index
c_p	Specific heat capacity of air (J kg^{-1} K^{-1})
CV	Coefficient of variation (%)
D	Air vapour pressure deficit (Pa)
ETo	Evapotranspiration
g_s	Stomatal conductance (mmol m^{-2} s^{-1})
$g_{s(dry\&wet)}$	Stomatal conductance calculated using both the wet and dry reference surfaces (mmol m^{-2} s^{-1})
$g_{s(dry)}$	Stomatal conductance calculated using the dry reference surface (mmol m^{-2} s^{-1})
$g_{s(no\ ref)}$	Stomatal conductance calculated without the use of reference surfaces (mmol m^{-2} s^{-1})
$g_{S(porometer)}$	Stomatal conductance as estimated using a porometer (mmol m^{-2} s^{-1})
HSV	Colour model based on hue, saturation, and value
I_G	Conductance index
MSX	FLIR proprietary image format
PLS	Partial least squares regression
r_{aW}	Leaf boundary layer resistance to water vapour (s m^{-1})
RGB	Colour model based on red, green, and blue light
RH	Relative humidity (%)
r_{HR}	Parallel resistance to heat and radiation transfer (s m^{-1})
R_{ni}	Net isothermal radiation (W m^{-1})
r_s	Stomatal resistance (s m^{-1})
s	Slope of the curve relating saturated water vapour pressure to temperature (Pa $°K^{-1}$)
SIM	Subscriber identity module
T_{air}	Air temperature (°C)
T_{canopy}	Canopy temperature (°C)
T_{dry}	Dry reference temperature (°C)
$T_{dry(fab)}$	Dry reference temperature obtained from a fabric surface (°C)
$T_{dry(leaf)}$	Dry reference temperature obtained from a detached leaf (°C)
$T_{dry(pet)}$	Dry reference temperature obtained by coating the leaf with petroleum jelly (°C)
T_{wet}	Wet reference temperature (°C)
$T_{wet(fab)}$	Wet reference temperature obtained from a damp fabric surface (°C)
$T_{wet(leaf)}$	Wet reference temperature obtained by spraying a leaf with water (°C)
VGA	Video graphics array
Wi-Fi	Wireless communication protocol
ρ	Density of air (kg m^{-3})
Υ	Psychrometric constant (Pa K^{-1})
Ψ_{stem}	Stem water potential (MPa)

1. Introduction

Smartphones contain or can be attached to a variety of sensors which have the potential to monitor the surrounding environment and provide an aid to decision making across a range of industries from medicine through to agriculture. Smartphones have a number of advantages over specialist monitoring systems including ubiquity, price, user familiarity and the ease of implementing updates; they also contain sufficient computing power that the analysis and support software can be contained within the phone (Ozdalga, Ozdalga, & Ahuja, 2012).

The measurement of water availability in the agricultural environment is important for the efficient use of a valuable and increasingly scarce resource (Gerten et al., 2011) and to obtain high quality produce (Fereres & Evans, 2006). There are a wide range of plant and soil water status assessment systems available for commercial use in Australia (Charlesworth, 2005; White & Raine, 2008), with soil-based sensors being by far the most popular in Australian viticulture, where use is reported by more than 60% of growers (Green & Griffante, 2009). Soil-based systems are often preferred in the commercial environment because of their robustness, minimal maintenance requirements, familiarity among users and suppliers and low skilled labour requirements once installed (Charlesworth, 2005). Unfortunately, soil-based sensing systems designed to measure to a depth (1 m and below) relevant for perennial crops, are point based and do not allow the variation in soil moisture across an orchard or vineyard to be easily assessed.

An easy, portable and cost-effective system for the direct and real-time assessment of plant water status remains a challenge for all agricultural industries (Jones, 2004). Plant-based monitoring systems are often used in a research context, unfortunately their application to commercial production has been limited (Naor, 2006). The direct indication of plant water status and ability to avoid symptoms that result in a reduction in productivity or quality are key positive attributes of measuring plant water status (Jones, 2004). Plant-based sensors are often far more portable so they can be easily moved between plants, allowing variation across a vineyard or orchard to be easily assessed.

Pre-dawn, leaf or stem water potential are the most widely accepted methods for the direct sensing of plant water status (Jones, 2004). There are several limitations to the commercial use of these techniques; including the extensive labour requirements, operator safety, inconsistency between operators and the requirement for leaf pre-bagging for stem water potential. An alternative plant-based method to assess crop water status is based on the measurement of the conductance of water vapour through the stomata. This can be completed by using a porometer or other devices that can measure the gas exchange of individual leaves; however, the logistics of measuring individual leaves across a canopy make these methods difficult (Costa, Grant, & Chaves, 2013).

Thermal imaging can be used as a surrogate for the direct measurement of water loss by leaves, based on the principle that the reduction in temperature is proportional to the rate of water loss due to the evaporative cooling process (Brown &

Escombe, 1905). Infrared thermometry was first developed as an indicator of plant water status in the 1960s (Tanner, 1963), and technological improvements over the last 50 or more years has allowed the refinement of these techniques for irrigation scheduling. Thermal cameras are now available that are integrated into or able to be connected directly to a smartphone. These systems can potentially be used to assess the irrigation requirements of crops and meet the portability and ease of use requirements for wide scale adoption. Interest in the use of thermal imaging to assess plant water status has increased as the price and size of the thermal cameras has decreased. This includes the use of ground-based and unmanned aerial vehicle-based systems to assess crop water status (e.g. Baluja et al., 2012; Bellvert et al., 2015; Grant, Ochagavía, Baluja, Diago, & Tardáguila, 2016), including the automated analysis of the thermal images (Fuentes, de Bei, Pech, & Tyerman, 2012; Gutierrez, Diago, Fernandez-Novales, & Tardaguila, 2018).

Different solutions have been developed to allow plant water status to be estimated from canopy temperature. A range of simple indices were created with a focus on generating values suitable for irrigation scheduling, such as the Crop Water Stress Index (CWSI) (Idso, 1982; Jones, 1999). These indices compared the temperature of the canopy with the temperatures of reference surfaces that represent the canopy of a well-watered and a drought stressed plant. More complex equations have been used to estimate stomatal conductance directly. However, as canopy temperature is not only affected by stomatal conductance and transpiration, but a range of other environmental variables such as air temperature, wind speed, radiation and humidity a range of external meteorological inputs are required (Alchanatis et al., 2010; Guilioni, Jones, Leinonen, & Lhomme, 2008; Leinonen, Grant; Tagliavia, Chaves, & Jones, 2006). The accuracy of these indices will vary with the environment and their utility will vary with both the accuracy and the number of external parameters that need to be collected to accurately assess plant water status.

This work was carried out to assess the accuracy of a consumer grade thermal camera and smartphone system for the assessment of grapevine water status in a commercial setting. Several components were systematically evaluated, in order to implement an optimal system:

1) Automatic selection of the canopy, and reference surfaces (if required);
2) Accuracy and precision of water stress indices relative to reference methods;
3) Impact of environmental conditions on accuracy of selected indices;
4) User acceptance of the integrated application.

2. Materials and methods

2.1. Trial site and sampling regime

Trial vines were located at the Loxton Research Centre in the Riverland region of South Australia. They consisted of a plot of Cabernet Sauvignon managed to four irrigation levels (namely 100%, 50%, 25% and 12.5% of evapotranspiration (ETo) throughout the season), and a plot of Chardonnay, both fully irrigated (100% ETo) and a deficit irrigation regime (25% ETo) imposed two weeks prior to the first assessments of vine water status. Each replicate comprised three adjacent rows of six adjacent vines, with the four central vines being the focus of measurements. The between-vine spacing for both the Chardonnay and Cabernet Sauvignon was 2 m and the between-row spacing was 3 m for the Chardonnay and 3.3 m for the Cabernet Sauvignon. Measurements of vine water status were collected on the six treatments (four Cabernet Sauvignon and two Chardonnay) on 30 different dates between December 2016 and March 2017. For each irrigation treatment, four assessments were made of T_{canopy}, T_{wet} and T_{dry} using the thermal camera, in conjunction with $g_{S(porometer)}$ readings from four shaded leaves and Ψ_{stem} from three leaves per treatment. All the assessments were averaged for each irrigation treatment by cultivar combination to give a total of 180 samples. The aim of sampling across multiple dates was to provide a wide range of weather conditions so the robustness of the thermal imaging technique could be assessed. Vine water status of the trial vines varied from well-watered to relatively stressed across treatments and measurement dates, with Mid-Day Stem Water Potential (Ψ_{stem}) ranging between −0.25 (Chardonnay, 100% irrigation) and −1.7 (Cabernet Sauvignon, 12.5% Et) MPa, and g_S ranging from 17 (Cabernet Sauvignon, 12.5% Et) to 530 (Chardonnay, 100% irrigation) mmol m^{-2} s^{-1}.

2.2. Stomatal conductance and stem water potential measurements

Two standard measures of vine water status were used. Ψ_{stem} was measured using a pressure chamber, model 3000 (Soil Moisture Equipment Corporation, Santa Barbara, CA, USA) with the standard analogue gauge replaced with a 0–5 MPa digital gauge (DG 25, Ashcroft, Stratford, Connecticut, USA). The method of Choné et al. (2001) was followed; briefly, leaves were enclosed in an aluminium foil covered bag for at least one hour prior to measurement so that leaf water potential could equilibrate with Ψ_{stem}. Stomatal conductance (g_S) was measured using a SC-1 Leaf Porometer (Decagon Devices, Pullman, Washington, USA), following the operating instructions for this device.

2.3. Meteorological data

Meteorological data were collected from the Natural Resources SA Murray-Darling Basin weather station at Loxton, which is located approximately 400 m from the trial site. The data available included air temperature, humidity, solar radiation wind speed and direction, and were available as 15-min averages which were synchronised with the collection of the thermal images.

2.4. Thermal imaging

The FLIR One (Wilsonville, Oregon, USA) thermal camera was selected for this project; it has a 160 by 120 pixel resolution.

The system includes a second VGA (640 by 480 pixel resolution) camera mounted adjacent to the thermal sensor, and software that generates an overlay which defines the border of the objects in the image making it easier to orientate and focus. The thermal images are stored, including the overlay, in the proprietary MSX image format. The camera has a long wave infrared sensor with a range from 8 to 14 μm, a thermal sensitivity better than 0.1 °C and the lens has a field of view of 46° horizontally and 35° vertically. The camera will measure over a temperature range of −20 °C to 120 °C with an accuracy of ±3 °C or ±5% (of the average of the difference between the ambient and the scene temperature) (Anon, 2015). For this work the emissivity was set at 0.95 and the distance to the focal plane set to 2 m. FLIR provides a software development kit to allow the development of applications in both iOS and Android operating systems.

2.5. Thermal indices and stomatal conductance estimation

The Crop Water Stress Index (CWSI) was calculated based on the equation modified from Idso (1982) by Jones (1999) for the use of wet and dry reference leaves:

$$CWSI = \frac{T_{canopy} - T_{wet}}{T_{dry} - T_{wet}} \quad (1)$$

where T_{canopy} is the shaded canopy temperature (°C) obtained from the thermal image (Pou, Diago, Medrano, Baluja, & Tardaguila, 2014), and T_{dry} and T_{wet} are the reference temperatures (°C). T_{dry} was obtained by either painting the abaxial side of the leaf with petroleum jelly ($T_{dry(pet)}$) (Vaseline, Unilever, London, U.K.) (Idso, 1982; Jones, 1999), using a 0.15 m diameter circular red fabric reference surface ($T_{dry(fab)}$) similar to Maes et al. (2016), or a leaf that had been detached for at least five minutes ($T_{dry(leaf)}$). A fresh leaf was painted with petroleum jelly prior to measurements being carried out on each treatment, while the same detached leaf was used for the series of measurements (up to two hours) on the corresponding cultivar. T_{wet} was the temperature of leaves sprayed with water and a little dishwashing soap during measurements ($T_{wet(leaf)}$) or using a fabric reference surface ($T_{wet(fab)}$) again similar to Maes et al. (2016), but coloured red. The leaves took approximately 30 s to cool once the water was applied and depending on ambient conditions would maintain a stable temperature for at least 60 s before they started to increase in temperature again (data not shown). A range of terrycloth fabrics were evaluated for the $T_{dry(fab)}$ and $T_{wet(fab)}$ during initial testing and significant differences in the relationship between fabrics and leaf-based reference surfaces were observed. To have a consistent supply of fabric that could be easily accessed by other growers or researchers, we selected a towel that was distributed globally (Fräjen, IKEA, Leiden, Netherlands) and represented the leaf-based reference surface appropriately.

The CWSI was also rearranged as proposed by Jones (1999) to give the conductance index (I_G):

$$I_G = \frac{T_{dry} - T_{canopy}}{T_{canopy} - T_{wet}} \quad (2)$$

where I_G is proportional to the stomatal conductance and therefore decreases as the stomata close and the differential between the T_{wet} and the T_{canopy} increases. As the CWSI and the I_G are derived from the same parameters, they are correlated. The relationship between CWSI and stomatal conductance is linear, but as the relationship between I_G and stomatal conductance is curvilinear, this index is more sensitive to changes in plant water status when the water deficit is low. This makes it more suitable for use in humid conditions or where less water stress is present (Jones, 1999).

A series of formulae has also been derived from the basic leaf energy balance (Jones et al., 2002) to calculate stomatal conductance (g_s) directly from canopy temperature and a combination of environmental variables and reference leaf temperatures (Guilioni et al., 2008; Leinonen, Grant, Tagliavia, Chaves, & Jones, 2006). These formulae potentially offer the advantage of allowing plant water status to be calculated based on meteorological parameters (collected by a weather station adjacent to site) without the requirement to erect the dry or the wet and the dry reference surfaces. By convention stomatal resistance (r_s) was calculated using mass units (s m^{-1}); however, its inverse g_s ($1/r_s$) is presented in molar units (mmol m^{-2} s^{-1}) using the conversion provided by Jones (2013).

Stomatal resistance (equation (3)) is calculated directly based on canopy temperature and environmental parameters (Leinonen et al., 2006):

$$r_s = -\rho \times c_p \times r_{HR} \times \left(s\left(T_{canopy} - T_{air}\right) + D\right) / \left(\gamma\left(T_{leaf} - T_{air}\right) \times \rho \times c_p - r_{HR} \times R_{ni}\right) - r_{aW} \quad (3)$$

where ρ is the density of air (kg m^{-3}), c_p is the specific heat capacity of air (J kg^{-1} K^{-1}), s is the slope of the curve relating saturated water vapour pressure to temperature (Pa K^{-1}), r_{HR} is the parallel resistance to heat and radiative transfer (s m^{-1}), D is the air vapour pressure deficit (Pa), Υ is the psychrometric constant (Pa K^{-1}), R_{ni} is the net isothermal radiation (the net radiation for a leaf at air temperature (W m^{-1})) and r_{aW} is the leaf boundary layer resistance to water vapour (s m^{-1}).

Equation (4) avoids the need for the measurement of adsorbed radiation by using T_{dry} (Leinonen et al., 2006):

$$r_s = -\rho \times c_p \times r_{HR} \times \left(s\left(T_{canopy} - T_{air}\right) + D\right) / \left(\gamma\left(T_{leaf} - T_{air}\right) \times \rho \times c_p \times \left(T_{canopy} - T_{dry}\right)\right) - r_{aW} \quad (4)$$

Complementing the above calculations; r_s can also be calculated based on environmental parameters and wet and dry reference surfaces. The most appropriate formula for our situation relates to a reference surface that is wet on both sides and a canopy comprising hypostomatous (stomata on the lower side) leaves (Guilioni et al., 2008).

$$r_s = \left(r_{aW}/2 + \left(s/\gamma\right) \times r_{HR}\right) \times \left(T_{canopy} - T_{wet}\right) / \left(T_{dry} - T_{canopy}\right) - r_{aW}/2 \quad (5)$$

2.6. Image capture and analysis

Images were collected approximately 1.5 m from the shaded side of the canopy for all measurements, as previous work by Pou et al. (2014) suggested that this would give the strongest

correlation with our reference methods. We also expected that this would allow the assessment of vine water status during intermittently cloudy conditions as rapid changes in the energy balance would not occur with fluctuating light levels. The canopy temperature and the wet and dry reference temperatures (both leaf and artificial reference) were manually extracted with the area selection and measurement tool from the images using the FLIR Tools software (Wilsonville, Oregon, USA).

For the automatic detection of the canopy temperature and wet and dry reference temperatures, the images were processed on the smartphone as follows. The 640 by 480 pixel thermal image in MSX format was processed using a 7 by 7 pixel Gaussian smoothing filter to reduce noise. To identify the wet and dry reference surfaces (approximately 100 pixels across), a binary reference mask corresponding to the red areas in the RGB image (the wet and dry references) was generated by converting the RGB (Red, Green, Blue) image to HSV (Hue, Saturation, Value) format and selecting the red portion of the image as having values, H: 328–366, S: 0.47–1.0 and V: 0.21–1.0. Noise (random variation across the binary image) was removed using two series of filters of different sizes. A 5 by 5 pixel erode filter and then a 7 by 7 pixel dilate filter were used to remove speckles followed by an 11 by 11 pixel erode filter and a 9 by 9 pixel dilate filter to close any gaps. The filter was also applied to the thermal image with a 15 pixel inset to avoid errors due to poor focus of the thermal image or misalignment of the original RGB and thermal images. The thermal data in the wet and dry references was divided into isotherms at 0.1 °C intervals and the temperature of the warmest (dry reference) and coldest (wet reference) isotherm, which was also greater than 50 pixels in size, was selected.

To calculate the canopy temperature, a second binary mask was created from the thermal image. All sections of the image that contained temperatures that were hotter than the dry reference and cooler than the wet reference were excluded (Fuentes et al., 2012). The image noise and potential errors due to poor focus were managed using the filters and inset described above. The mask to delineate both the reference surfaces and the canopy were applied to the RGB image and displayed on the screen of the smartphone to allow the user to check that the image processing had worked and correctly highlighted the appropriate areas.

The canopy temperature was automatically calculated from the portion of the image remaining once the masks had been used to exclude the image background and the reference surfaces. Once again, a 15-pixel inset was used to avoid errors due to poor focus of the thermal image or misalignment of the original RGB and thermal images.

2.7. Data processing and analysis of accuracy and precision

All results were collated in Microsoft Excel 2016 (Microsoft, Redmond, Washington, USA); the ordinary least squares regression analysis and the calculation of the coefficient of variation were completed using Minitab 18 (State College, Pennsylvania, USA). For the regression the continuous predictor was the reference method (Ψ_{stem} and g_S) and the response was the thermal indices (CWSI and I_G) or stomatal conductance estimation ($g_{s(no\ ref)}$, $g_{s(dry)}$, and $g_{s(dry\&wet)}$). Prior to calculating the coefficient of variation, the data were normalised by dividing each individual sample by the mean for its corresponding sample date and treatment and then multiplying the result by the population mean. The aim of normalising the data was to remove the variation due to sample date and treatment, while maintaining the variation between samples. This analysis included the 720 individual samples across the season, from four measurements per replicate, for $g_{S(porometer)}$, CWSI, I_G, and on 540 samples from three measurements per replicate for Ψ_{stem}. The coefficient of variation was not calculated for the other indices as the weather data included in their calculations was averaged over 15 min which meant the variation between individual samples could not be captured.

Partial least squares (PLS) regression was completed using The Unscrambler X (CAMO Software, Gaustadalléen, Norway) to investigate the impact of the environment (air temperature, relative humidity, incident radiation and average wind speed) on the relationship between $g_{S(porometer)}$ and Ψ_{stem}, and CWSI and I_G. The data were standardised to prevent the model variables with the larger range having a disproportionate impact on the model, and a two-component model was selected for the PLS regression in all cases. PLS regression was used as co-linearity was expected between the weather parameters, especially RH and T_{air}, and this would prevent them being distinguished as causes of error in the relationships between the reference methods (Ψ_{stem} and g_S) and the thermal indices (CWSI and I_G). The residuals from the ordinary least squares regression between the reference methods (Ψ_{stem} and g_S) and the thermal indices (CWSI and I_G) were modelled using the environmental parameters as these were a convenient measure of error in the original relationships.

2.8. User acceptance testing

Preliminary trials suggested that the CWSI would be the most suitable index for the assessment of vine water status (Skewes, Petrie, Liu, & Whitty, 2018) and an application was developed on this basis. An alternate index (e.g. I_G) could have been introduced to the application during the season if improvements in accuracy or ease of use had warranted it. The 16 reviewers were selected from attendees at an industry conference who volunteered to participate. They were chosen to cover a broad range of geography, environment and operation size to ensure we covered both owner operators and corporate vineyards. The average age was approximately 41 and there were four females in the review group. The reviewers received the system midway through the 2016-17 season and were encouraged to make assessments of water status as part of their normal vineyard visits. A system was distributed to the reviewers comprising the FLIR One, an Android Smartphone (A1601, Oppo, Dongguan, Guangdong, China), the reference surfaces and comprehensive instructions on the operation of the application and the interpretation of the results. Briefly; broad guidelines on using CWSI were provided to the reviewers based on the recommendations of Deloire and Rogiers (2014) and the existing relationship between Ψ_{stem} and CWSI (Skewes et al., 2018);

and they were encouraged to investigate sections of their vineyards that were not monitored by their existing soil-based measurement systems. The reviewers were recommended to benchmark their readings at a similar time of the day and to be aware that the environmental conditions will influence the results; as occurs with all plant-based sensing systems. The reviewers were also asked to use the system as a supplement to their current irrigation scheduling practises, but major practise change was not expected within the four months of the trial. No formal program of use or systematic evaluation of the accuracy of the system was required and none of the reviewers regularly used any plant-based method for assessing water status. The user acceptance testing was conducted in order to receive feedback on the concept and application interface as opposed to refining irrigation scheduling practises.

The application was configured to automatically synchronise measurements with a server every time the phone was connected to Wi-Fi (a SIM card was not installed), as this allowed camera usage to be tracked and diagnostics easily provided for any user issues. The application and its instructions were refined and updated throughout the 2016-17 growing season, with updates to the application being made when the phones were connected to Wi-Fi. Analysis of the images collected by the review group suggested that they were not using a 'slider bar' that had been provided to help improve the accuracy of the canopy selection. The algorithm to select the canopy was improved, so this feature could be removed from the application. Changes in the CWSI formula to account for improvement in calculating the relationships between the $T_{dry(pet)}$ and $T_{dry(fab)}$, and $T_{wet(leaf)}$ and $T_{wet(fab)}$ were also made during the season. After harvest the user acceptance testers were surveyed about the utility of the application and their intentions for further use if it was made publicly available: the questions asked in the survey are presented in Table 1. The survey was followed up by telephone or in-person interview to capture more specific comments or suggestions for improvements.

Table 1 – Responses of the user acceptance testers (n = 16) to statements regarding the performance of the application and questions on intentions for future use.

Statement number	Summary of survey statements	Strongly Disagree	Disagree	Neutral	Agree	Strongly Agree
1	The App was simple to use	0%	0%	0%	75%	25%
2	The methodology for using the app is clearly defined in the instructions	6%	0%	13%	56%	25%
3	I was comfortable installing the reference leaves for each set of measurements	13%	6%	25%	50%	6%
4	The CWSI results were what you expected	6%	0%	19%	63%	13%
5	I considered the weather conditions when making measurements and interpreting results	0%	6%	19%	38%	38%
6	The CWSI figures were useful in making irrigation decisions	0%	0%	38%	50%	13%
7	Would you consider using the app in the future?	13%	n/a	6%	n/a	81%
8	Would you recommend the app to others?	0%	n/a	12%	n/a	88%

3. Results

3.1. *Automatic selection of the canopy and reference surfaces*

The reliable selection of the canopy, so that T_{canopy} can be determined, and the accurate assessment of T_{dry} and T_{wet} are critical to the accurate calculation of g_s and the water stress indices. Two systematic comparisons were made. The first was to check the reliability of the canopy selection by comparing canopy temperatures calculated from a manually selected portion of the canopy with the fully automated selection. A strong, 1:1 relationship was seen between the manual selection and fully automated methods (Fig. 1).

The second assessment was to determine the accuracy of using artificial T_{dry} and T_{wet} as substitutes for leaves treated with sprayed water or petroleum jelly. The temperature of the $T_{dry(pet)}$ was used as the benchmark comparison to the temperature of the $T_{dry(fab)}$ and the $T_{dry(leaf)}$. Once again, a strong relationship was seen between the $T_{dry(pet)}$ and both the

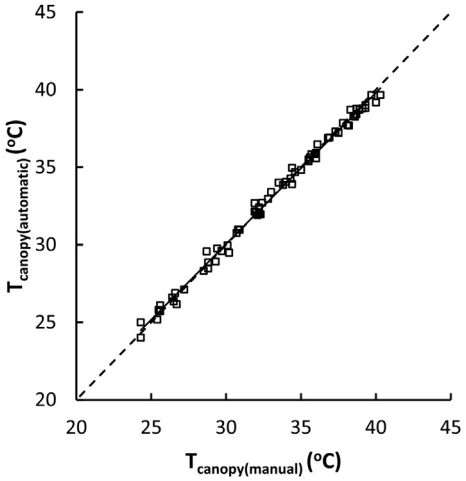

Fig. 1 – The relationship between the temperature of a manually selected section of the grapevine canopy ($T_{canopy(manual)}$) and the temperature of the entire canopy selected automatically by the application ($T_{canopy(automatic)}$); $R^2 = 0.99$, RMSE = 0.327, $T_{canopy(automatic)} = 0.792 + 0.97541\ T_{canopy(manual)}$, $P < 0.001$. All measurements were taken from the shaded side of the canopy. Dashed line is 1:1.

$T_{dry(fab)}$ and the $T_{dry(leaf)}$ (Fig. 2a, b). The relationship was not 1:1 between $T_{dry(pet)}$ and the $T_{dry(leaf)}$, with the $T_{dry(leaf)}$ averaging 0.6 °C higher than the $T_{dry(pet)}$ ($P < 0.001$). There was similar variation in temperature for all the T_{dry} references (standard deviation 5.28–5.43 °C). The relationship between $T_{wet(leaf)}$ and $T_{wet(fab)}$ was not as strong as between the dry temperature references, however the R^2 was above 0.87. Once again, the slope was not 1:1, with the $T_{wet(fab)}$ averaging 2.2 °C less than $T_{wet(leaf)}$ ($P < 0.001$) (Fig. 3). The temperature of the $T_{wet(fab)}$ (standard deviation, 3.35 °C) appeared to be more stable than the $T_{wet(leaf)}$ (standard deviation, 4.01 °C). As the relationship between the leaf and the fabric-based T_{dry} and T_{wet} was not 1:1, all the fabric reference temperatures were adjusted using the relationships reported in Figs. 2 and 3 prior to the calculation of indices.

Further investigations were conducted into the effect of the environment on the stability of $T_{wet(leaf)}$ and $T_{wet(fab)}$. An attempt was made to determine the impact of the exposure time required for the $T_{wet(fab)}$ to equilibrate with the environment. By the time the wet reference surface was transported into position in the canopy from a hot vehicle or a refrigerator (approximately 30 s) the temperature was similar to a second wet reference that was already located in the canopy. A shorter integration time was not attempted as for practical purposes this was sufficient. Likewise, if the $T_{wet(fab)}$ was to dry out under ambient conditions this would lead to inaccurate results. The temperature variation across the $T_{wet(fab)}$ (as an indication the upper part of the reference was drying) was assessed under a range of conditions and the only time a variation was noted was under hot and dry conditions, when a fan was used to blow air across the target. A similar response was seen by a researcher who was testing the app in an enclosed and heated chamber used to simulate warmer conditions, due to climate change. In this case, water needed to be regularly sprayed on the $T_{wet(leaf)}$ during the calibration.

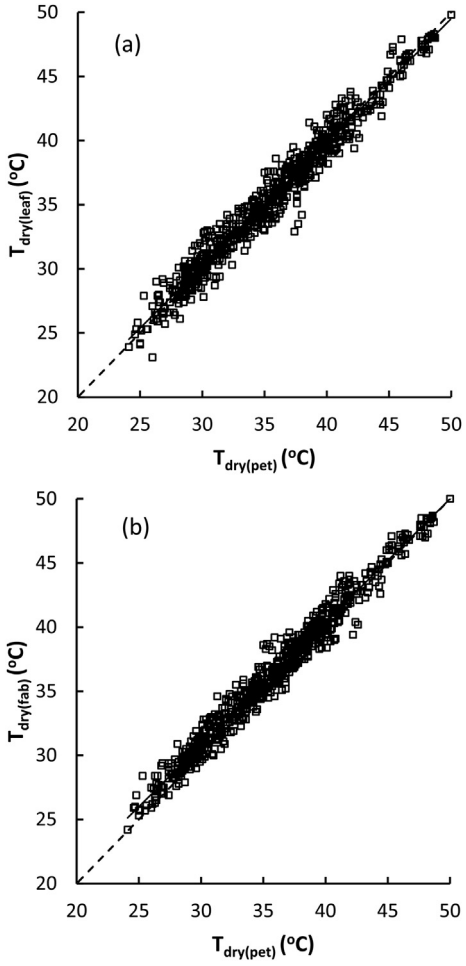

Fig. 2 – The relationship between the temperature of the leaf with the abaxial side coated with petroleum jelly ($T_{dry(pet)}$) with: (a) the temperature of a detached leaf that was suspended in the canopy ($T_{dry(leaf)}$); $R^2 = 0.97$, RMSE = 0.988, $T_{dry(leaf)} = 1.246 + 0.96515\ T_{dry(pet)}$; $P < 0.001$. (b) the temperature of the fabric reference surface ($T_{dry(fab)}$); $R^2 = 0.97$, RMSE = 0.848, $T_{dry(fab)} = 2.004 + 0.95984\ T_{dry(pet)}$; $P < 0.001$. All measurements were taken under shaded conditions. Dashed line is 1:1.

The water was maintained on the leaf for over 150 s under cool (wet leaf temperature 10–14 °C) and still conditions, but the leaf would begin to dry in less than 90 s under warm (wet leaf temperature 20–24 °C) and windy conditions (data not shown).

3.2. *Accuracy and precision relative to reference methods*

Indices calculated from the canopy temperature were compared to both the g_S measured using a porometer and Ψ_{stem} (Figs. 4a–e and 5a–e). The relationships between $g_{S(porometer)}$ and the indices was linear (Fig. 4a–e), while the relationships between Ψ_{stem} and the indices were best predicted using a curvilinear models (Fig. 5a–e). The CWSI showed the strongest relationships with both $g_{S(porometer)}$ and Ψ_{stem} (Figs. 4a and 5a) and the relationship between

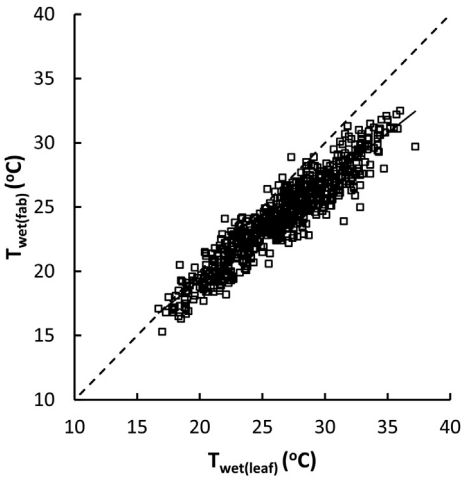

Fig. 3 – The relationship between the temperature of the leaf where the adaxial surface had been sprayed with water ($T_{wet(leaf)}$) and the wet fabric reference surface ($T_{wet(fab)}$); $R^2 = 0.88$, RMSE = 1.18, $T_{wet(fab)} = 3.968 + 0.7656\ T_{wet(leaf)}$, $P < 0.001$. All measurements were taken under shaded conditions. Dashed line is 1:1.

$g_{S(porometer)}$ and the index was always stronger than the relationship between Ψ_{stem} and the equivalent index. Of the indices designed to estimate stomatal conductance, I_G and $g_{s(dry)}$ were the best performing but none showed a 1:1 relationship with $g_{S(porometer)}$ (Fig. 4c–e).

The CWSI was surprisingly stable with a coefficient of variation of 3.5%, while the I_G was more variable with a coefficient of variation of 16%. The reference methods ($g_{S(porometer)}$ and Ψ_{stem}) also exhibited some variation; the coefficient of variation for the stomatal conductance was 21%; while for Ψ_{stem} it was a lot less (5%).

3.3. *Impact of environmental conditions on accuracy*

The sample conditions under which the relationships between the indices and the reference methods were calculated intentionally included some challenging conditions (Table 2). On a clear day the incident radiation at this site is often above 1000 W m^{-2} during the summer; many of the values are markedly below this (Table 2) indicating that some cloud cover was present on most of the days when samples were collected. On the 30 January 2017 the conditions were humid and on the 22 February 2017 the conditions were windy. We would not normally recommend growers assess water stress under these conditions and when the 12 samples collected across the two days were excluded the relationships between the reference methods and the indices generally improved; for example, the relationship between $g_{S(porometer)}$ and CWSI improved from $R^2 = 0.74$, to $R^2 = 0.80$.

Partial least squares (PLS) regression was used to further investigate the impact of the environment (air temperature, relative humidity, incident radiation and average wind speed) on the relationship between both $g_{S(porometer)}$ and Ψ_{stem}, and CWSI and I_G. The PLS regression was used to model the relationship between environmental parameters and the residuals from the relationships presented in Figs. 4a, b and 5a, b. As expected, PLS regression models were weak (Table 3) with all the R^2 below 0.32. Most of the weather parameters made a statistically significant contribution to the PLS models, the only exceptions were for RH for the residuals from the $g_{S(porometer)}$:I_G relationship and T_{air} for the Ψ_{stem}:I_G relationship. Wind speed was consistently the strongest contributor to uncertainty across all relationships (Table 3).

3.4. *User acceptance*

Each reviewer used the system on an average of approximately 50 occasions (range 17–160). Most users found the application simple to use (statement 1, Table 1) and the instructions easy to follow (statement 2). They generally felt that the results (CWSI) were what they expected (statement 4) and we took this to mean they reflected the appearance of the vines or their other measurements of water status (primarily soil moisture content). Informal feedback, either written comments or by phone, suggested that the unusually wet season in some testing locations meant that vines didn't experience the usual level of water stress, which limited some of the opportunities to test the application. There was less certainty about the utility of the CWSI for scheduling irrigation (statement 6), but none of the testers disagreed with this question. Comments from the interviews suggested that once the users became more familiar with the application and the CWSI as a method for assessing vine water status, the confidence in this technique would improve. The primary areas of concern for the testers were the need to collect images from the shaded side of the row and the requirements to erect the $T_{dry(fab)}$ and $T_{wet(fab)}$ in the canopy for each reading (statement 3). Several users suggested improvements to the mounting or display of the $T_{dry(fab)}$ and $T_{wet(fab)}$ which are easy to implement, others requested that a system be developed that doesn't require the reference surfaces. These methods were investigated further as part of this project (see above). Over 80% of the testers would consider using the application in the future and recommend it to others to use (statements 7 and 8).

4. Discussion

The development of a method to accurately automate the extraction of the canopy temperature from its surroundings in an image was key to a system that could be easily used in the field. This area has been the subject of previous research (Wang, Yang, Wheaton, Cooley, & Moran, 2010a; 2010b), and we successfully built on the concepts developed by Fuentes et al. (2012). Initially the application allowed the manual adjustment of the proportion of the canopy that was used to assess temperature, however this proved difficult to use in the field and the improvement of the canopy detection algorithm meant that it was no longer necessary (Fig. 1).

The requirement to apply petroleum jelly and water to leaves prior to collecting thermal images was unlikely to be appealing to growers, especially as the water application was only maintained for up to 90 s under our conditions. Maes et al. (2016) tested a green fabric-based reference in glasshouses and vineyards and found it gave better relationships between $g_{S(porometer)}$ and I_G than I_G calculated from the

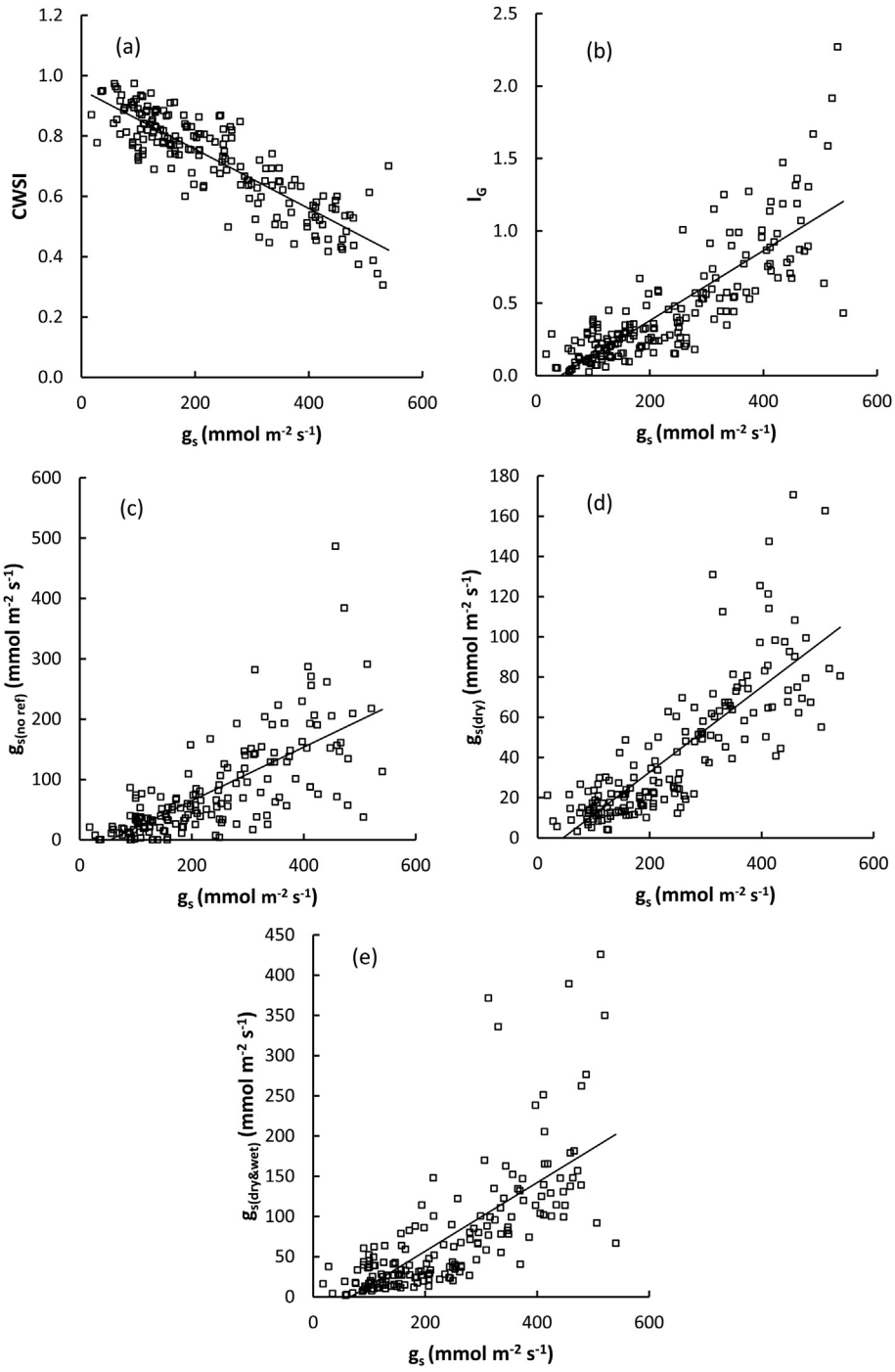

Fig. 4 – The relationship between stomatal conductance (g_s) averaged from four porometer readings taken from individual leaves of Chardonnay and Cabernet Sauvignon subject to a range of water deficit treatments (see section 2.6 for details) on 30 days across the 2016–17 growing season (n = 186) and: (a) Crop Water Stress Index calculated from the average canopy temperature and the wet ($T_{wet(fab)}$) and dry ($T_{dry(fab)}$) fabric reference surfaces, $R^2 = 0.74$, RMSE = 0.0767, CWSI = 0.9528–0.000982 g_s, P < 0.001; (b) Conductance index (I_G) calculated from the average canopy temperature and the wet ($T_{wet(fab)}$) and dry ($T_{dry(fab)}$) fabric reference surfaces, $R^2 = 0.68$, RMSE = 0.00242, $I_G = -0.1033 + 0.002418\ g_s$, P = 0.000; (c) Stomatal conductance ($g_{s(no\ ref)}$) calculated from the average canopy temperature and environmental parameters (see text for details), $R^2 = 0.52$, RMSE = 55.5, $g_{s(no\ ref)} = -24.13 + 0.4445\ g_s$, P = 0.000; (d) Stomatal conductance ($g_{s(dry)}$) calculated from the average canopy temperature, environmental parameters and the dry fabric reference surface ($T_{dry(fab)}$), $R^2 = 0.67$, RMSE = 19.1, $g_{s(dry)} = -9.60 + 0.2115\ g_s$, P = 0.000; and (e) Stomatal conductance ($g_{s(dry\&wet)}$) calculated from the average canopy temperature, environmental parameters and the wet ($T_{wet(fab)}$) and dry ($T_{dry(fab)}$) fabric reference surfaces, $R^2 = 0.52$, RMSE = 52.8, $g_{s(dry\&wet)} = -28.47 + 0.4268\ g_s$, P = 0.000. All measurements were taken under shaded conditions and the portion of the canopy used for the temperature readings was automatically selected by the application (see text for details). Note that the scales for g_s on the y axis are not consistent.

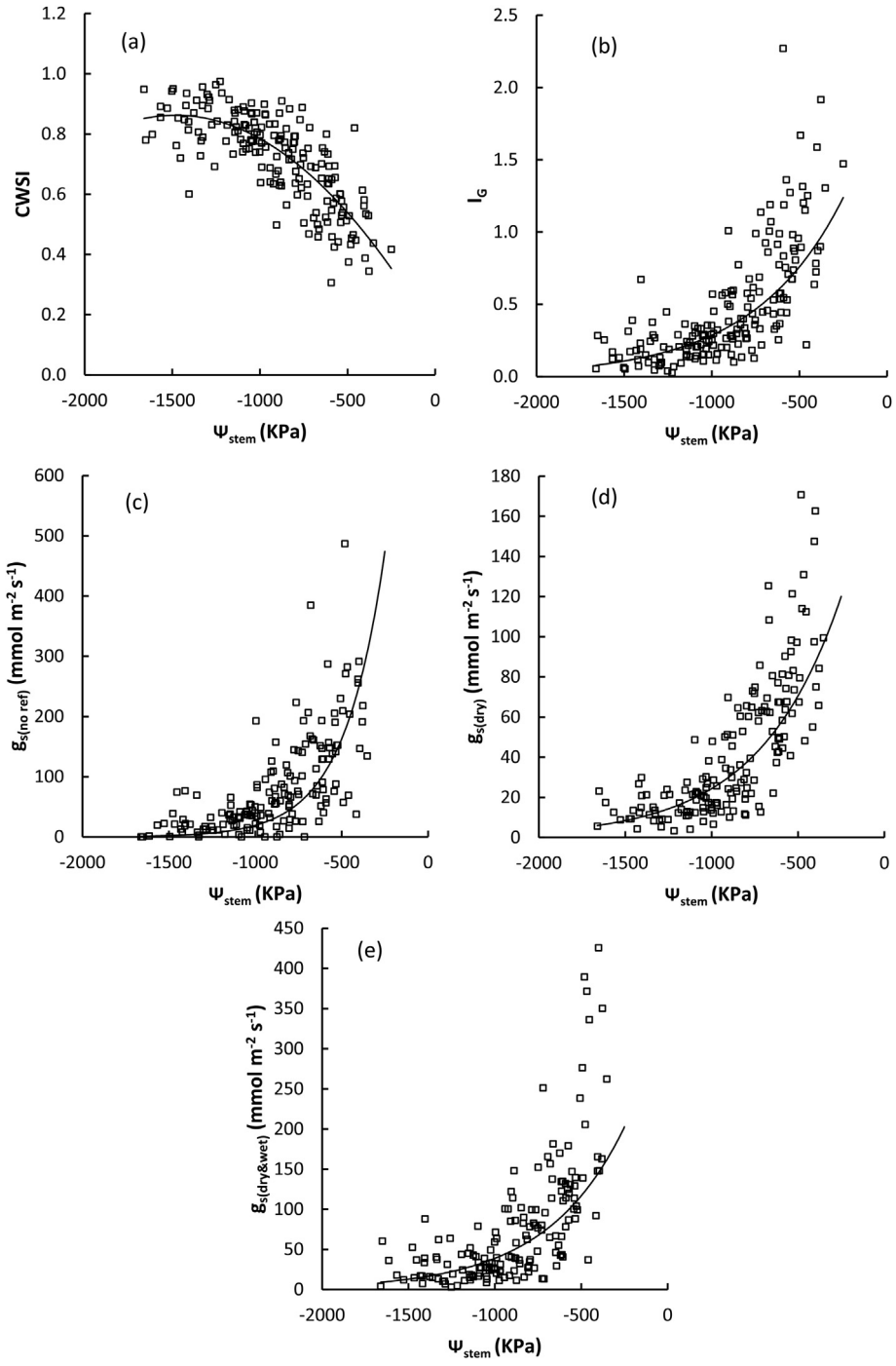

Fig. 5 – The relationship between stem water potential (Ψ_{stem}) averaged from three leaves of Chardonnay and Cabernet Sauvignon subject to a range of water deficit treatments (see section 2.6 for details) on 30 days across the 2016–17 growing season (n = 180) and: (a) Crop Water Stress Index calculated from the average canopy temperature and the wet ($T_{wet(fab)}$) and dry ($T_{dry(fab)}$) fabric reference surfaces, $R^2 = 0.61$, RMSE = 0.100, CWSI = 0.1247–0.000996 Ψ_{stem} – 0.00000003 Ψ^2_{stem}, $P < 0.001$; (b) Conductance index (I_G) calculated from the average canopy temperature and the wet ($T_{wet(fab)}$) and dry ($T_{dry(fab)}$) fabric reference surfaces, $R^2 = 0.55$, RMSE = 0.284, $I_G = 2.74922\ e^{0.00218463\ \Psi stem}$, P = 0.000; (c) Stomatal conductance ($g_{s(no\ ref)}$) calculated from the average canopy temperature and environmental parameters (see text for details), $R^2 = 0.42$, RMSE = 61.4, $g_{s(no\ ref)} = 558.714\ e^{0.00239234\ \Psi stem}$, P = 0.000; (d) Stomatal conductance ($g_{s(dry)}$) calculated from the average canopy temperature, environmental parameters and the dry fabric reference surface ($T_{dry(fab)}$), $R^2 = 0.61$, RMSE = 22.7, $g_{s(dry)} = 268.682\ e^{0.00233211\ \Psi stem}$, P = 0.000; and (e) Stomatal conductance ($g_{s(dry\&wet)}$) calculated from the average canopy temperature, environmental parameters and the wet ($T_{wet(fab)}$) and dry ($T_{dry(fab)}$) fabric reference surfaces, $R^2 = 0.48$, RMSE = 59.6, $g_{s(dry\&wet)} = 757.889\ e^{0.00301378\ \Psi stem}$, P = 0.000. All measurements were taken under shaded conditions and the portion of the canopy used for the temperature readings was automatically selected by the application (see text for details). Note that the scales for g_s on the y axis are not consistent.

Table 2 – Meteorological conditions[a] and sample times for the thirty days when plant water status measurements were collected.

Date	Time of first reading[b]	Time of last reading[c]	Average T_{air} (°C)	Average RH (%)	Average Incident Radiation (W m^{-2})	Average wind speed (km hr^{-1})
19/12/2016	1:38 PM	3:16 PM	36 (35.3, 37.1)	11.3 (10.9, 12.2)	705 (184, 952)	5.8 (3.7, 9)
21/12/2016	12:38 PM	3:00 PM	27.2 (26.2, 28)	26.1 (24.1, 29.4)	880 (734, 1057)	11.3 (10.3, 12.9)
10/01/2017	1:15 PM	3:04 PM	32.8 (32.7, 32.9)	36.2 (35.3, 37)	781 (398, 1009)	8.7 (6.7, 11)
12/01/2017	1:43 PM	3:55 PM	35.1 (34.2, 35.8)	20.5 (19.6, 21.6)	693 (514, 889)	5.2 (3, 7.7)
16/01/2017	1:40 PM	3:29 PM	36.1 (35.4, 36.6)	12.5 (11.8, 13.4)	829 (660, 954)	5.4 (3.2, 8.3)
17/01/2017	1:08 PM	3:24 PM	42.4 (41.8, 43)	5.7 (4.9, 6.4)	846 (656, 1027)	10.1 (5.9, 16.8)
23/01/2017	12:38 PM	2:06 PM	38.4 (36.3, 39.4)	18.6 (16.7, 21.2)	568 (290, 932)	14 (8.1, 19.6)
25/01/2017	12:06 PM	2:20 PM	28.1 (26.9, 29)	24.4 (21.9, 27.9)	963 (827, 1090)	8.4 (6.4, 10.7)
30/01/2017[d]	12:59 PM	2:52 PM	32.2 (31.6, 32.7)	41.3 (46.1, 50.9)	285 (173, 401)	11.2 (7.2, 13.3)
1/02/2017	12:22 PM	2:29 PM	27.4 (26.9, 27.6)	27.9 (27.1, 29.4)	657 (436, 999)	6.4 (4.2, 8.5)
7/02/2017	12:47 PM	2:50 PM	28.1 (27, 29.3)	48.6 (39.3, 43.2)	849 (678, 981)	8 (7.1, 8.9)
8/02/2017	12:20 PM	2:14 PM	41 (39.8, 41.7)	23.6 (22, 25.5)	887 (784, 991)	9.6 (7.8, 11.4)
9/02/2017	12:22 PM	2:25 PM	45.1 (44, 45.9)	12.3 (11.2, 13.3)	768 (503, 1016)	9.5 (6, 12.8)
13/02/2017	12:28 PM	2:20 PM	24.7 (23.5, 25.4)	39.4 (38.1, 41.8)	886 (770, 1011)	14.5 (11.2, 16.5)
14/02/2017	12:56 PM	2:58 PM	27.8 (27.1, 28.7)	25.5 (23.4, 26.8)	767 (646, 983)	4.9 (2.4, 6.2)
15/02/2017	12:29 PM	2:27 PM	35.3 (34.4, 35.9)	14.4 (13.3, 15.6)	813 (715, 877)	14.1 (12.9, 16.3)
16/02/2017	12:26 PM	2:20 PM	29.9 (28.6, 31.3)	39.5 (35.5, 42.7)	879 (626, 993)	7.6 (4.1, 11.1)
20/02/2017	12:33 PM	2:52 PM	22.8 (21.9, 23.6)	28.2 (26.9, 30.2)	840 (683, 987)	9.4 (5.8, 12)
22/02/2017[d]	12:37 PM	2:53 PM	36.7 (36.5, 37.1)	11.2 (10.6, 12.5)	856 (638, 983)	16.7 (13.9, 19.2)
23/02/2017	12:37 PM	2:50 PM	26.2 (24.9, 27.6)	38.1 (32.8, 42.6)	877 (661, 1035)	8 (7.2, 8.9)
24/02/2017	12:37 PM	2:39 PM	26.1 (25.2, 26.9)	28.2 (27.4, 29.2)	877 (707, 991)	13.3 (10.4, 15.3)
27/02/2017	12:34 PM	2:33 PM	35.9 (35.4, 36.4)	22.2 (21.5, 24.8)	558 (419, 778)	6.2 (3.8, 8.9)
28/02/2017	12:32 PM	2:39 PM	36.4 (36.2, 36.7)	16.3 (15.2, 17.1)	849 (697, 937)	8.8 (7.2, 10.4)
2/03/2017	12:45 PM	2:40 PM	36.2 (35.7, 36.6)	17.2 (16.6, 17.7)	635 (209, 1057)	10.2 (7.1, 12.2)
6/03/2017	12:32 PM	2:26 PM	30.4 (30, 30.8)	29.4 (27.5, 30.9)	549 (318, 712)	7.8 (6.9, 9.2)
7/03/2017	12:38 PM	2:45 PM	33.7 (33.1, 34.1)	18 (17.2, 19.8)	468 (246, 708)	7.9 (6, 9.8)
8/03/2017	1:05 PM	2:51 PM	34 (33.3, 34.7)	20.1 (19, 22.4)	445 (178, 650)	5.6 (3.6, 8.4)
9/03/2017	1:06 PM	3:05 PM	33 (30.5, 35.2)	23.6 (15, 32)	255 (63, 577)	2.9 (0.4, 6.5)
14/03/2017	12:42 PM	2:46 PM	31.6 (31, 31.9)	27.2 (26.5, 28.4)	466 (210, 670)	9.7 (8.1, 10.7)
20/03/2017	12:54 PM	2:48 PM	33.7 (32.2, 35.2)	28.1 (24.7, 32)	360 (81, 560)	3.5 (2.1, 5)

[a] Meterological values are an average of the six 15-min averages during which each of the individual thermal images were collected.
[b] Denotes time when first thermal image was collected; Australian Central Standard Time.
[c] Denotes time when last thermal image was collected.
[d] Denotes the dates for which the data was excluded from the relationship between $g_{S(porometer)}$ and CWSI to improve the relationship between these variables (see section 3.3 for details).

Table 3 – The weighted regression coefficients for the partial least squares (PLS) regression model of the residuals from the ordinary least squares regression between $g_{S(porometer)}$ and Ψ_{stem} and CWSI and I_G (see Figs. 4a, b and 5a, b) and the environmental variables; air temperature, relative humidity, solar radiation, and wind speed. Standard errors are presented in square brackets, except when the weighted regression coefficients were not significant; when they were denoted with ns.

	CWSI	I_G
$g_{S(porometer)}$		
R^2	0.32	0.23
Air Temperature (°C)	0.0175 [0.00875]	−0.0339 [0.0237]
Relative Humidity (%)	−0.0106 [0.00813]	0.0229 [ns]
Solar Radiation (W m^{-2})	−0.0225 [0.00969]	0.0492 [0.0288]
Wind Speed (km hr^{-1})	0.0325 [0.0109]	−0.0915 [0.0356]
Ψ_{stem}		
R^2	0.20	0.14
Air Temperature (°C)	0.56 [0.0083]	−0.8 [ns]
Relative Humidity (%)	−0.86 [0.00906]	1.9 [0.0281]
Solar Radiation (W m^{-2})	−1.26 [0.0143]	2.9 [0.04]
Wind Speed (km hr^{-1})	1.52 [0.0117]	−4.5 [0.0342]

traditional $T_{dry(pet)}$ and $T_{wet(leaf)}$. While we didn't investigate this directly, the standard deviation of the $T_{wet(leaf)}$ was higher than the $T_{wet(fab)}$ in our work, which suggests the temperature of this reference was more stable and likely to lead to more consistent relationships. The leaves of Chardonnay and Cabernet Sauvignon are contrasting in texture and both were used to develop the leaf and the fabric-based T_{dry} and T_{wet} so we would expect this relationship would hold for other cultivars of *Vitis vinifera*, but this was not assessed. Further calibration may be needed for *Vitis labrusca* or other crop species.

Red fabric was selected for the references, so this could be easily identified by the software application. The matching of the colour and colour density of the reference surface to the crop is potentially important so that they have a similar response to the environment, especially incident radiation (Jones et al., 2009). By focussing the measurements (and the reference surfaces) on the shaded side of the canopy, where the incident radiation is lower, the potential for differences in response of the canopy and reference surface was reduced (Jones et al., 2002), meaning that stronger relationships between the fabric and leaf references were maintained (Figs. 2 and 3).

The strength of the relationships we observed between the reference methods ($g_{S(porometer)}$ and Ψ_{stem}) and the indices (CWSI, I_G, $g_{s(no\ ref)}$, $g_{s(dry)}$ and $g_{s(dry\&wet)}$) (Figs 4 and 5) were similar to other authors using manual and automated image processing and thermal cameras with better specifications (e.g. (Fuentes et al., 2012; Jones et al., 2002; Leinonen et al., 2006; Pou et al., 2014)). Like other authors working in arid climates, the CWSI gave the best relationships with $g_{S(porometer)}$ and Ψ_{stem} (Pou et al., 2014) compared to other potential indices. Given that the reference methods also include some measurement error (CV of 5–21%), the R^2 of the relationship between the CWSI and $g_{S(porometer)}$ ($R^2 = 0.74$) suggests that this method is suitable for making irrigation decisions in the field. This conclusion is supported by other authors for olive (Ben-Gal et al., 2009), peach (Park et al., 2017), almond (Garcia-Tejero et al., 2018), cotton (Cohen et al., 2017; O'Shaughnessy, Evett, & Colaizzi, 2015) and potato (Rud et al., 2014) as well as grapevines (Fuentes et al., 2012; Möller et al., 2007; Pou et al., 2014). Garcia-Tejero et al. (2018) have recently evaluated the same model of thermal camera (FLIR One) for the assessment of water status of almond trees. The smartphone-based camera overestimated canopy temperature relative to a higher resolution camera; however, a strong relationship between leaf water potential and CWSI could still be demonstrated.

Indices have been developed that reduce or negate the requirements for the reference surfaces (Guilioni et al., 2008; Gutierrez et al., 2018; Leinonen et al., 2006) and in some cases these have recorded a similar accuracy to indices derived from wet and dry reference surfaces (Leinonen et al., 2006). As the need to install the reference surfaces is a potential barrier to the widespread adoption of this technique by vineyard managers, we evaluated a range of indices with different input requirements and targeting different conditions. An external weather station (portable or installed at a vineyard site) could provide the necessary parameters directly to the mobile phone to allow the indices to be calculated. Unfortunately, the relationships between the indices that didn't require some or all of the reference surfaces ($g_{s(no\ ref)}$ and $g_{s(dry)}$) and the reference methods was not as strong as with the CWSI. When no reference surfaces were used the R^2 of the relationship between $g_{s(no\ ref)}$ and $g_{S(porometer)}$ was approximately 0.5 and with Ψ_{stem} was closer to 0.4; this suggests that assessing vine water status based only on the thermal camera and meteorological conditions wasn't accurate enough for irrigation scheduling under our conditions; this has been seen by other authors (Alchanatis et al., 2010; Cohen et al., 2015). The relationship between the $g_{s(dry)}$ and $g_{S(porometer)}$ was a little better ($R^2 = 0.67$) but not as good as the CWSI; we felt that the loss in accuracy did not justify the omission of the wet reference, especially as the dry reference was still required. If a system based on a permanently installed camera was used to supply a continuous stream of data that may be easier to interpret, then an index that only requires the dry reference may be more suitable. This was recently proposed for a system using a IR sensor, as opposed to a camera (Jones, Hutchinson, May, Jamali, & Deery, 2018). Some of the reduction in accuracy of indices that rely on input from the external weather station may be due to the poor accuracy of the FLIR One thermal camera (±3 °C) leading to inconsistency with the values collected from the weather station. The reduced accuracy is a key difference between professional grade thermal cameras and the consumer cameras used in this study. The weather sensors also had an integration time of 15 min, meaning that the 15 min average value may not correspond well with the instantaneous temperatures collected by the thermal camera.

Environmental conditions affect the accuracy of the indices, however the broader the conditions that vine water status can be assessed over the more likely the method will be adopted by growers. To reduce the potential impact of overcast conditions or intermittent cloud cover, the system was developed and calibrated over a range of conditions (Table 2), based on images taken from the shaded side of the canopy. Results from the sun-exposed side of the canopy are likely to be more sensitive to changes in vine water status as the difference in temperature between T_{wet} and T_{dry} is larger under direct light (Jones, 1999). However Pou et al. (2014), working in a similar arid environment, observed a stronger relationship between stomatal conductance and both CWSI and I_G, when the images were collected from the shaded side of the canopy. Agam, Cohen, Alchanatis, and Ben-Gal (2013) suggested that intermittent cloud can disrupt the calculation of the CWSI, especially in water-stressed plants with low transpiration rates; however, we did not observe this in our results. This is likely to be due to our canopy measurements focussing on the shaded side of the canopy where the impact of rapid changes in available energy are less. In addition, we used a fabric T_{dry} as opposed to a T_{dry} calculated as 5 °C greater than T_{air}. The temperature of the fabric T_{dry} may have been more dynamic in its response to changes in environmental conditions and therefore allowed the CWSI to better track g_s.

Sub-optimal conditions can affect the accuracy of the indices, for example humid conditions reduce the temperature differential between T_{wet} and T_{dry} as less evaporative cooling occurs (Jones et al., 2002) and windy conditions can change the canopy energy balance (Jones et al., 2002) as well as stimulating stomata to close (Campbell-Clause, 1998). To investigate this further, the relationship between the residuals from the calibration of the $g_{S(porometer)}$ and Ψ_{stem} against CWSI and I_G (see Figs. 4a, b and 5a, b) and weather conditions was modelled using partial least squares regression. While all the weather parameters (air temperature, relative humidity, incident radiation and average wind speed) potentially impacted on the precision of the indices, wind speed consistently had the largest effect (Table 3). There is increased uncertainty with results when the wind speed was greater than approximately 13 km h^{-1}; which was one standard deviation greater than the mean wind speed seen in this trial and a similar minimum speed to the windy day that was excluded from the analysis (see section 3.3).

Refinements were able to be made during the application development and testing phase to address feedback from the test users. The demand for a smartphone-based system that could assess plants directly was demonstrated by the positive responses to the potential uses for this application (Table 1). We were aware that the need to use the shaded side of the row and to install the $T_{dry(fab)}$ and $T_{wet(fab)}$ would be a potential barrier to some users. Unfortunately, our testing suggests that

these components are essential to the accurate measurement of vine water status.

5. Conclusions

A range of methods are available to assess vine water status and aid in making irrigation decisions – however none currently meet the portability and ease of use requirements for wide scale adoption. The system we developed based on a smartphone and a thermal camera appears to be sufficiently accurate and easy to use that it is likely to be widely adopted. This will provide vineyard managers with better information on the water status of their vineyards, which in turn will allow better irrigation decisions to be made to improve the use of irrigation water and produce higher quality fruit.

Acknowledgements

The authors gratefully acknowledge the support of Mr Gary Grigson and the farm staff at the SARDI Loxton Research Centre for the maintenance of the irrigation trial; the helpful discussions and input from Drs Marcos Bonada and Everard Edwards during this project; and the assistance from Dr Bob Dambergs with the partial least squares regression.

This work was supported by Australian grapegrowers and winemakers through their investment body Wine Australia (SAR 1501 Smartphone based image analysis to assess vine water stress), with matching funds from the Australian Government. The Australian Wine Research Institute and the South Australian Research and Development Institute are members of the Wine Innovation Cluster in Adelaide.

REFERENCES

Agam, N., Cohen, Y., Alchanatis, V., & Ben-Gal, A. (2013). How sensitive is the CWSI to changes in solar radiation? *International Journal of Remote Sensing, 34*(17), 6109–6120.

Alchanatis, V., Cohen, Y., Cohen, S., Moller, M., Sprinstin, M., Meron, M., et al. (2010). Evaluation of different approaches for estimating and mapping crop water status in cotton with thermal imaging. *Precision Agriculture, 11*(1), 27–41.

Anon. (2015). *FLIR one for Android/iOS*. Wilsonville, Oregon, USA: FLIR Systems Inc.

Baluja, J., Diago, M. P., Balda, P., Zorer, R., Meggio, F., Morales, F., et al. (2012). Assessment of vineyard water status variability by thermal and multispectral imagery using an unmanned aerial vehicle (UAV). *Irrigation Science, 30*(6), 511–522.

Bellvert, J., Zarco-Tejada, P. J., Marsal, J., Girona, J., González-Dugo, V., & Fereres, E. (2015). Vineyard irrigation scheduling based on airborne thermal imagery and water potential thresholds. *Australian Journal of Grape and Wine Research, 22*(2), 307–315.

Ben-Gal, A., Agam, N., Alchanatis, V., Cohen, Y., Yermiyahu, U., Zipori, I., et al. (2009). Evaluating water stress in irrigated olives: Correlation of soil water status, tree water status, and thermal imagery. *Irrigation Science, 27*(5), 367–376.

Brown, H. T., & Escombe, F. (1905). Researches on some of the physiological processes of green leaves, with special reference to the interchange of energy between the leaf and its surroundings. *Proceedings of the Royal Society of London Series B, 76*(507), 29–111.

Campbell-Clause, J. M. (1998). Stomatal response of grapevines to wind. *Australian Journal of Experimental Agriculture, 38*(1), 77–82.

Charlesworth, P. (2005). *Soil water monitoring* (Vol. 1). Canberra, Australia: Land and Water Australia.

Choné, X., Leeuwen, C. V., Dubourdieu, D., Gaudillère, J.-P., van Leeuwen, C., Dubourdieu, D., et al. (2001). Stem water potential is a sensitive indicator of grapevine water status. *Annals of Botany, 87*(4), 477–483.

Cohen, Y., Alchanatis, V., Saranga, Y., Rosenberg, O., Sela, E., & Bosak, A. (2017). Mapping water status based on aerial thermal imagery: Comparison of methodologies for upscaling from a single leaf to commercial fields. *Precision Agriculture, 18*(5), 801–822.

Cohen, Y., Alchanatis, V., Sela, E., Saranga, Y., Cohen, S., Meron, M., et al. (2015). Crop water status estimation using thermography: Multi-year model development using ground-based thermal images. *Precision Agriculture, 16*(3), 311–329.

Costa, J. M., Grant, O. M., & Chaves, M. M. (2013). Thermography to explore plant-environment interactions. *Journal of Experimental Botany, 64*(13), 3937–3949.

Deloire, A., & Rogiers, S. (2014). Monitoring vine water status: Part 2 – A detailed example using the pressure chamber. In D. Fahey (Ed.), *Grapevine management guide 2014–15* (pp. 16–19). New South Wales Department of Primary Industries.

Fereres, E., & Evans, R. G. (2006). Irrigation of fruit trees and vines: An introduction. *Irrigation Science, 24*(2), 55–57.

Fuentes, S., de Bei, R., Pech, J., & Tyerman, S. (2012). Computational water stress indices obtained from thermal image analysis of grapevine canopies. *Irrigation Science, 30*(6), 523–536.

Garcia-Tejero, I. F., Ortega-Arevalo, C. J., Iglesias-Contreras, M., Moreno, J. M., Souza, L., Tavira, S. C., et al. (2018). Assessing the crop-water status in Almond (Prunus dulcis Mill.) trees via thermal imaging camera connected to smartphone. *Sensors (Basel), 18*(4), 1050.

Gerten, D., Heinke, J., Hoff, H., Biemans, H., Fader, M., & Waha, K. (2011). Global water availability and requirements for future food production. *Journal of Hydrometeorology, 12*(5), 885–899.

Grant, O. M., Ochagavía, H., Baluja, J., Diago, M. P., & Tardáguila, J. (2016). Thermal imaging to detect spatial and temporal variation in the water status of grapevine (Vitis vinifera L.). *The Journal of Horticultural Science and Biotechnology, 91*(1), 43–54.

Green, J., & Griffante, D. (2009). *Australian wine industry stewardship 2009 national report*. Kent Town, Adelaide: Winemakers' Federation of Australia.

Guilioni, L., Jones, H. G., Leinonen, I., & Lhomme, J. P. (2008). On the relationships between stomatal resistance and leaf temperatures in thermography. *Agricultural and Forest Meteorology, 148*(11), 1908–1912.

Gutierrez, S., Diago, M. P., Fernandez-Novales, J., & Tardaguila, J. (2018). Vineyard water status assessment using on-the-go thermal imaging and machine learning. *PLoS One, 13*(2), e0192037.

Idso, S. B. (1982). Non-water-stressed baselines: A key to measuring and interpreting plant water stress. *Agricultural Meteorology, 27*(1), 59–70.

Jones, H. G. (1999). Use of infrared thermometry for estimation of stomatal conductance as a possible aid to irrigation scheduling. *Agricultural and Forest Meteorology, 95*(3), 139–149.

Jones, H. G. (2004). Irrigation scheduling: Advantages and pitfalls of plant-based methods. *Journal of Experimental Botany, 55*(407), 2427–2436.

Jones, H. G. (2013). Heat, mass and momentum transfer. In H. G. Jones (Ed.), *Plants and microclimate: A quantitative approach to environmental plant physiology* (3 ed., pp. 47–67). Cambridge: Cambridge University Press.

Jones, H. G., Hutchinson, P. A., May, T., Jamali, H., & Deery, D. M. (2018). A practical method using a network of fixed infrared sensors for estimating crop canopy conductance and evaporation rate. *Biosystems Engineering, 165*, 59–69.

Jones, H. G., Serraj, R., Loveys, B. R., Xiong, L., Wheaton, A., & Price, A. H. (2009). Thermal infrared imaging of crop canopies for the remote diagnosis and quantification of plant responses to water stress in the field. *Functional Plant Biology, 36*(11), 978–989.

Jones, H. G., Stoll, M., Santos, T., de Sousa, C., Chaves, M. M., & Grant, O. M. (2002). Use of infrared thermography for monitoring stomatal closure in the field: Application to grapevine. *Journal of Experimental Botany, 53*(378), 2249–2260.

Leinonen, I., Grant, O. M., Tagliavia, C. P. P., Chaves, M. M., & Jones, H. G. (2006). Estimating stomatal conductance with thermal imagery. *Plant Cell and Environment, 29*(8), 1508–1518.

Maes, W. H., Baert, A., Huete, A. R., Minchin, P. E. H., Snelgar, W. P., & Steppe, K. (2016). A new wet reference target method for continuous infrared thermography of vegetations. *Agricultural and Forest Meteorology, 226–227*, 119–131.

Möller, M., Alchanatis, V., Cohen, Y., Meron, M., Tsipris, J., Naor, A., et al. (2007). Use of thermal and visible imagery for estimating crop water status of irrigated grapevine. *Journal of Experimental Botany, 58*, 827–838.

Naor, A. (2006). Irrigation scheduling and evaluation of tree water status in deciduous orchards. *Horticultural Reviews, 32*, 111–165.

O'Shaughnessy, S. A., Evett, S. R., & Colaizzi, P. D. (2015). Dynamic prescription maps for site-specific variable rate irrigation of cotton. *Agricultural Water Management, 159*, 123–138.

Ozdalga, E., Ozdalga, A., & Ahuja, N. (2012). The smartphone in medicine: A review of current and potential use among physicians and students. *Journal of Medical Internet Research, 14*(5), e128.

Park, S., Ryu, D., Fuentes, S., Chung, H., Hernández-Montes, E., & O'Connell, M. (2017). Adaptive estimation of crop water stress in nectarine and peach orchards using high-resolution imagery from an unmanned aerial vehicle (UAV). *Remote Sensing, 9*(8), 828.

Pou, A., Diago, M. P., Medrano, H., Baluja, J., & Tardaguila, J. (2014). Validation of thermal indices for water status identification in grapevine. *Agricultural Water Management, 134*, 60–72.

Rud, R., Cohen, Y., Alchanatis, V., Levi, A., Brikman, R., Shenderey, C., et al. (2014). Crop water stress index derived from multi-year ground and aerial thermal images as an indicator of potato water status. *Precision Agriculture, 15*(3), 273–289.

Skewes, M., Petrie, P. R., Liu, S., & Whitty, M. (2018). Smartphone tools for measuring vine water status. *Acta Horticulturae, 1197*, 53–58.

Tanner, C. B. (1963). Plant temperatures. *Agronomy Journal, 55*(2), 210–211.

Wang, X., Yang, W., Wheaton, A., Cooley, N., & Moran, B. (2010a). Automated canopy temperature estimation via infrared thermography: A first step towards automated plant water stress monitoring. *Computers and Electronics in Agriculture, 73*, 74–83.

Wang, X., Yang, W., Wheaton, A., Cooley, N., & Moran, B. (2010b). Efficient registration of optical and IR images for automatic plant water stress assessment. *Computers and Electronics in Agriculture, 74*, 230–237.

White, S., & Raine, S. R. (2008). *A grower guide to plant based sensing for irrigation scheduling*. Toowoomba, Australia: National Centre for Engineering in Agriculture, University of Southern Quensland.